A PLATFORM FOR IN SITU, REAL-TIME MEASUREMENT OF ELECTROCHEMICAL REACTION-INDUCED STRESS/STRAIN IN LITHIUM-ION BATTERY ELECTRODES

S. Baron*, E. Pomerantseva*, M. Gnerlich, K. Gerasopoulos, H. Jung, and R. Ghodssi
MEMS Sensors and Actuators Laboratory (MSAL)
Department of Electrical and Computer Engineering
Department of Materials Science and Engineering
Institute for Systems Research, University of Maryland, College Park, MD 20742, USA

Abstract: We report the first successful demonstration of the sensing capabilities of an optical MEMS platform for *in situ* characterization of electrochemically-induced reversible mechanical changes in lithium-ion battery (LIB) electrodes. The platform consists of an array of flexible membranes that deflect due to the active battery material volume change caused by lithium intercalation (expansion) and extraction (contraction). Membrane deflection is monitored using the Fabry-Perot optical interferometry principle. Developed platform opens new ways for *in situ* diagnostics of thin-film LIB electrodes to aid with the development of new materials, optimization of electrode performance, and prevention of battery failure.

Keywords: lithium-ion battery, electrode, volume expansion, Fabry-Perot interferometer

INTRODUCTION

Lithium-ion batteries (LIBs) have received a great deal of interest during the past years as they offer higher energy densities compared to other rechargeable battery systems while being compact and lightweight. Silicon is one of the promising electrode materials due to its exceptionally high theoretical capacity (~4200 mAh/g) [1]. However, silicon goes through significant volumetric expansion and contraction (~300%) as lithium is transported into and out of the electrode. The volumetric change during LIB's charge/discharge process is important since these volumetric excursions lead to stress/strain which can cause mechanical failure of the electrodes, decreasing battery capacity and eventually causing the battery to become unusable. Therefore, in order to closely monitor volumetric change at specific charge/discharge moment, new *in situ* materials characterization tools need to be developed for deeper understanding of the material property changes during electrochemical processes in LIB electrodes. Here we present a Fabry-Perot (FP) sensing platform that detects thin film silicon electrode volume changes during electrochemical cycling.

The platform consists of an array of flexible membranes, each located at the bottom of a vacuum sealed cavity formed between anodically bonded silicon and Pyrex wafers (Fig. 1). Membrane deflection is monitored using the FP optical interferometry principle. A gap between the Pyrex surface and the silicon nitride membrane creates a FP cavity. This gap dynamically changes due to stress in the thin-film stack resulting from active battery material expansion/contraction during lithium cycling (Fig. 2).

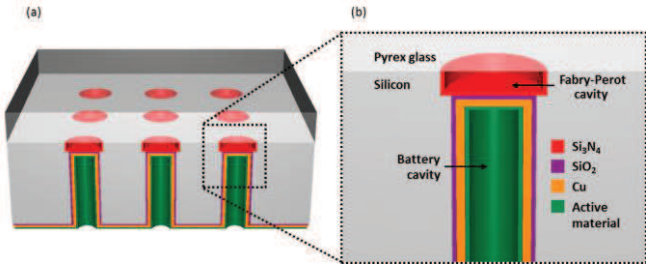

Fig. 1. 3D and cross-section diagrams of FP sensing platform design.

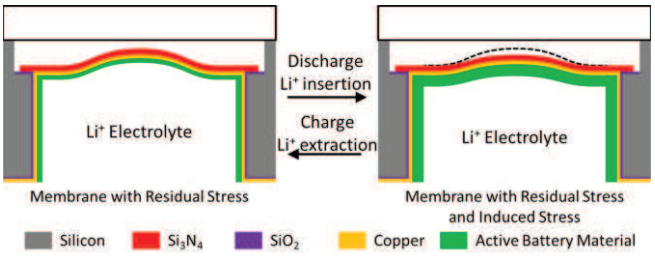

Fig. 2. Cross-section diagram of the principle behind the sensing mechanism of the FP platform. Monochromatic light is shone through the Pyrex top layer to create optical interference in the upper cavity, which is observable as a set of light and dark fringes.

MATERIALS AND METHODS

Simulation

As the active battery material expands/contracts, this volume change induces reversible membrane

*These authors contributed equally to this work.

deflection. The membrane deflection along the radius is described in Eq. 1. In this equation W is the membrane deflection, r is the specific point along the membrane radius, P is the applied pressure on the membrane, R_0 is the radius of the membrane, and D is the flexural rigidity (Eq. 2.), which is a combination of Young's modulus (E), Poisson's ratio (v) and thickness of the membrane (h). The deflection along the radius of the membrane due to volumetric expansion and contraction as lithium is cycled can be modeled as behavior of a circular plate with clamped edge under uniform loading with small deflection model [2] with radius (R_0).

$$W(r) = \frac{PR_0^4}{64D}\left[1 - \left(\frac{r}{R_0}\right)^2\right]^2 \quad (1)$$

$$D = \frac{Eh^3}{12(1-v^2)} \quad (2)$$

When a light source illuminates the FP cavity, the light is reflected and intensity of the reflected light changes according to the deflection of the membrane. According to FP interferometry principle, reflected light intensity due to membrane deflection is described by Eq. 3 [3]. The reflected light intensity, I, is a function of the finesse of the cavity, F, and the constant, K, calculated by Eq. 4, where d, θ, and λ are FP cavity depth, angle of the incident light source, and wavelength of the light source, respectively.

$$I = \frac{F\sin\left(K^2/_2\right)}{1 + F\sin\left(K^2/_2\right)} \quad (3)$$

$$K = \frac{4\pi d}{\lambda}\cos\theta \quad (4)$$

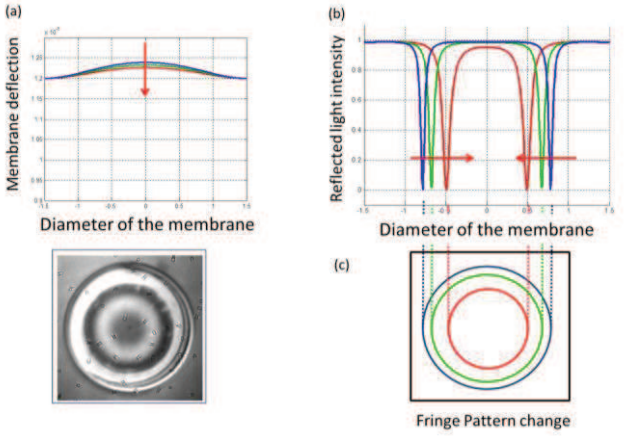

Fig. 3. Color-coded diagrams of the calculated results for membrane with residual stress: (a) membrane deflection, (b) intensity change, (c) FP pattern change. The inset shows an experimentally obtained FP fringe pattern.

FP cavity depth (d) can be replaced by Eq. 1. The constant K is derived by combining Eq. 1 and Eq. 4 as shown in Eq. 5, which allows the reflected light intensity (I) to be a function of membrane radius (r).

$$K = \frac{4\pi}{\lambda}W(r)\cos\theta \quad (5)$$

Using Eq. 1, the deflection profile according to different membrane deflection can be simulated by MATLAB (Fig. 3 (a)). At each membrane deflection, reflected intensity of a light along the membrane can be calculated using Eq. 3 and Eq. 5 and it is shown in Fig. 3 (b). The fringe pattern can be drawn using reflected light intensity (Fig. 3 (c)). This simulation results show that when membrane deflection is negative, fringe radius becomes smaller which is in good agreement with our experimental results described below.

Device Fabrication

Silicon wafers (double-side polished, 100 mm diameter, nominally 495–505 µm thick, (100) orientation) were used as substrates for the FP sensing

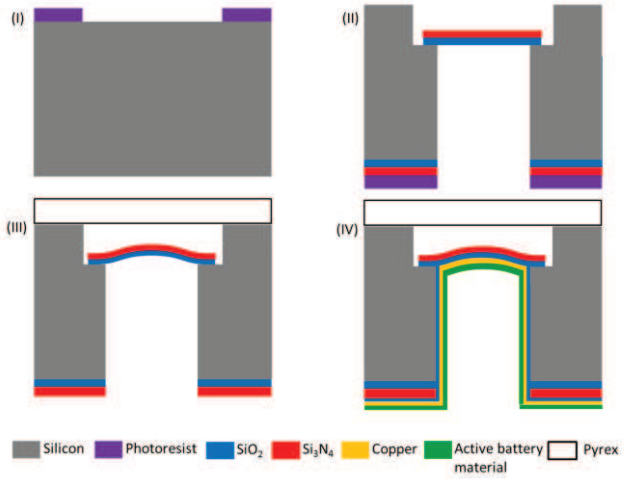

Fig. 4. Schematic presentation of the fabrication process of FP sensing platform.

platform fabrication. A gap between the Pyrex glass and the silicon nitride membrane (150 µm, 200 µm, 250µm and 300 µm in diameter) creates a FP cavity. The FP cavity (12 µm deep) is created using deep reactive ion etching (DRIE). The battery cavity (488 µm deep) is formed by backside DRIE. After the fabrication of the FP and battery cavities, Pyrex glass is anodically bonded on top of the FP cavity side. This is followed by thin-film deposition on the battery side of the device (Fig. 1(b)). A SiO_2 passivation layer (200 nm), which prevents Li intercalation into bulk Si, is formed by PECVD, while Cu current collector (250 nm) and Si electrode (1 µm) are deposited using

sputtering. A schematic presentation of the fabrication process of the FP sensing platform is shown in Fig. 4. The Cu current collector was sandwiched between Ti layers (5-20 nm) serving as adhesion layer between Cu and SiO_2 and preventing Cu from oxidizing prior to silicon sputtering. When combined with Li-conducting electrolyte and metallic Li as counter electrode in a coin cell package, this side of the device forms a lithium half-cell or battery system. Fig. 5 shows SEM images of the FP and battery cavities formed by DRIE.

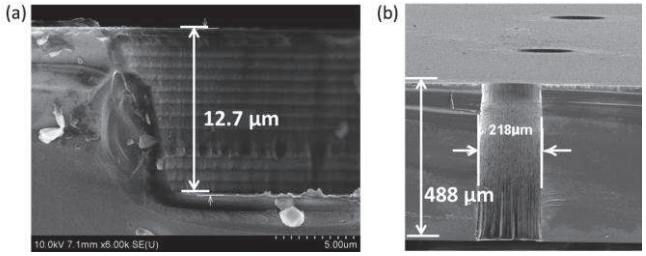

Fig. 5. SEM images of (a) FP cavity and (b) battery cavity.

Testing Apparatus

The FP sensing platform is diced into 1cm by 1cm chips and each chip is packaged in a modified coin cell as shown in Fig 6. A window in the coin cell cap was punched to enable optical measurements. Double-sided adhesive copper tape is applied in order to achieve hermetic sealing for the cell and good electron transport. On top of the copper tape, the diced chip is attached with the battery cavity facing inside a coin cell. The cell is assembled inside an Argon filled glove box.

The packaged FP sensing platform is placed on top of an optical microscope and connected to a battery testing station (Arbin Instruments, TX, USA) for lithium electrochemical cycling test as shown in Fig. 7. During the test, despeckled red laser light (660 nm) illuminates the FP cavity. The resulting FP pattern changes due to deflection of the membrane is monitored by a CCD camera. The experimentally achieved FP pattern is shown on the computer monitor in the inset of Fig. 7. The fringe pattern was recorded as a time-stamped image captured by the camera every 30 seconds.

RESULTS AND DISCUSSION

Galvanostatic lithium cycling experiment is conducted using the Arbin battery test station in the voltage range of 0.01V - 1.5V with the current density of 40 µA. Changes in the FP interference pattern occur over long time scales, where a single battery cycle may take several hours. Measurements over

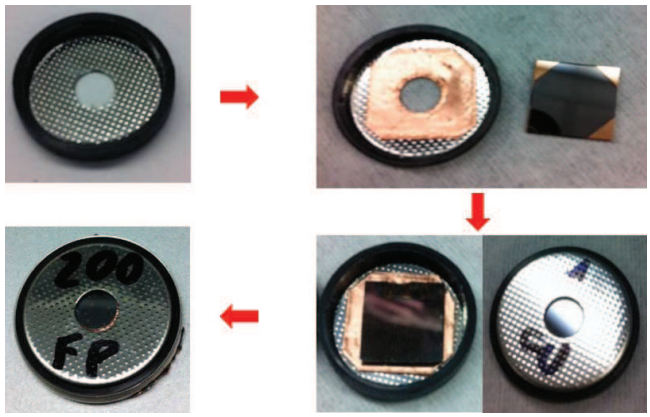

Fig. 6. Packaging process of FP platform inside a coin cell with the window using double-sided adhesive copper tape.

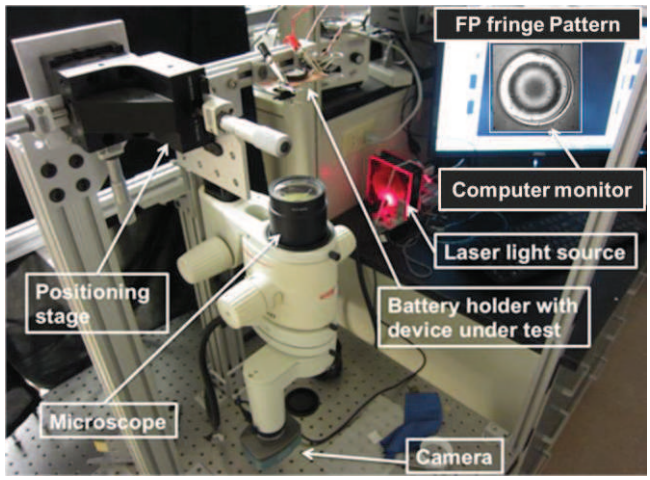

Fig. 7. Photograph of a complete experimental setup.

numerous cycles can produce thousands of images taken many days apart. To analyze the data, computerized image processing is necessary to handle the information. After time-stamped image capture, the image stack is preprocessed (e.g. normalization, and registration correction) and analyzed in MATLAB. Since the observed phenomenon is radially symmetric, the image data is converted from Cartesian (x,y) to polar (r,θ) coordinates. The angle (θ) information for a constant radius (r) is averaged together to produce a plot of light intensity as a function of radial distance from the center of the image. This effectively oversamples the fringe position by combining independent measurements of its position, each at different angle from the center of the image. Next, two features are algorithmically detected from the intensity plot: (1) the center fringe is identified as the local minima with lowest radial distance, and (2) the edge of the cavity is identified as the local minima with highest radial distance. Finally, the center fringe position can be measured relative to the immovable edge of the cavity in order to prevent a

drift in the position of the sample. It is then plotted as a function of time where the measurement at *t=0* is defined as zero measured shift (Fig. 8).

Upon lithium intercalation, the active battery material expands and causes the membrane to deflect away from the Pyrex surface. The membranes with pristine silicon electrodes are pre-stressed as a result of processing conditions (Fig. 4). The flattening of the membranes causes a decrease in the observed number and radii of FP fringes. Shape change of the membrane is reversed during lithium extraction, which was confirmed by both simulations (Fig. 3) and experimental testing (Fig 8). These results are in good agreement with previously reported data for thin-film silicon electrodes [4,5]. Upon lithium intercalation the silicon film initially deforms elastically, resulting in rapid decrease of FP fringe radius. This follows by lithiated silicon being deformed plastically under compressive stress, which corresponds to the constant FP fringe radius. Upon lithium extraction, the electrode first undergoes elastic straining in the opposite direction (increase of FP fringe radius) leading to a tensile stress; subsequently it deforms plastically during the rest of the charge (Fig. 9).

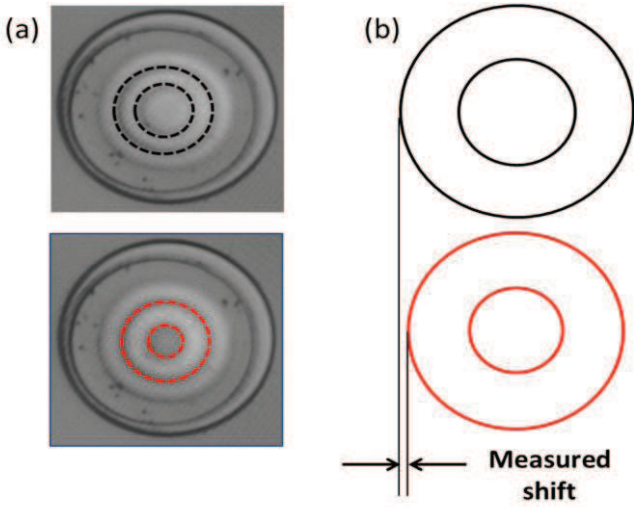

Fig. 8. (a) Photographs of experimentally obtained fringe patterns and (b) corresponding diagram for "measured shift".

CONCLUSION

In this work we have for the first time demonstrated sensing capabilities of the MEMS Fabry-Perot membrane-based platform for *in situ* characterization of electrochemically induced stress/strain in thin film LIB electrodes. The membrane deflection is induced by silicon thin film electrode volume expansion/contraction during electrochemical cycling. This developed sensing technology enables *in situ* characterization of various thin film LIB electrodes and leads to better understanding of electrochemically driven stress generation, deformation and fracture causing degradation and failure of batteries.

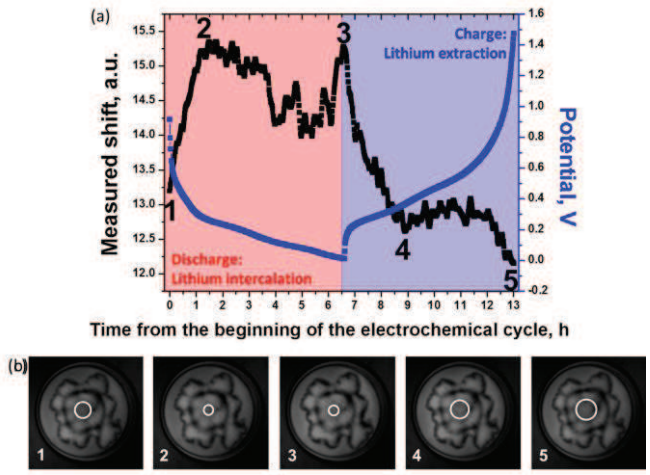

Fig. 9. (a) Correlation between FP fringe pattern change and electrochemical cycling of 1μm thick silicon electrode. FP images corresponding to time points 1-5 are shown in (b). The central fringe, which showed largest movement, is highlighted.

ACKNOWLEDGEMENTS

This work was supported by the Nanostructures for Electrical Energy Storage, an Energy Frontier Research Center funded by the U.S. Department of Energy, Office of Science, Office of Basic Energy Sciences under Award Number DESC0001160. The authors acknowledge the staff at Maryland Nanocenter.

REFERENCES

[1] Szczech J R, Jin S 2011 *Energy & Environmental Science* **4** 56-72.

[2] Timoshenko S P, Woinowsky-Krieger S 1959 *Theory of plates and shells, 2nd ed*. (New York, McGraw-Hill).

[3] Hernandez G 1986 *Fabry-Perot Interferometers* (New York, Cambridge University Press).

[4] Vijay A S, Michael J C, Maxwell S, Venkat S, Pradeep R G 2010 *J. Power Sources* **195** 5062-5066.

[5] Vijay A S, Michael J C, Maxwell S, Venkat S, Pradeep R G 2010 *Electrochemical Communications* **12** 1614-1617.